4) What does the vector A_0A represent?

5) What does the vector B_0B represent?

6) What does the vector C_0C represent?

Using the data in Figure 4.11, calculate:

7) $\tan \alpha$.

8) $\tan \beta$.

9) $u_1(x_1+d\,x_1, x_2) - u_1(x_1, x_2)$ and give an interpretation of this result.

10) $u_2(x_1+d\,x_1, x_2) - u_2(x_1, x_2)$ and give an interpretation of this result.

11) $u_1(x_1, x_2+d\,x_2) - u_1(x_1, x_2)$ and give an interpretation of this result.

12) $u_2(x_1, x_2+d\,x_2) - u_2(x_1, x_2)$ and give an interpretation of this result.

13) Calculate the components of the tensor based on elongations per unit length. Give the expressions of this tensor denoted by e_{ij}.

14) In the case of an overall rotation of the plane with an angle δ without strain, calculate the components of the tensor.

15) Prove that the second rank tensor T_{ij} can be written in the form of a symmetric tensor S_{ij} and of an antisymmetric tensor A_{ij}.

16) Give the expressions of S_{ij} and A_{ij} in the case of tensor e_{ij}.

17) Provide an interpretation of the terms S_{ij} and A_{ij}.

4.4.1.1.*Solutions*

1) Recall the principle of the model used for the calculation of the strain tensor using Figure 4.11 as a reference.

Solutions:

The hypothesis of the continuous medium is generally adopted in order to describe the strain of a material. At a point of the material localized by a

vector **r**, which in 2D has the components x_1 and x_2 and located at point A in the figure, consider small displacements represented by a translation vector **u(r)**, which is represented by vector A_0A in the figure.

During the deformation of the material, the variations of $u_1(x_1, x_2)$ along x_1 and x_2 are evaluated, as the quantities $du_1(x_1, x_2) = (\partial u_1/\partial x_1)dx_1 + (\partial u_1/\partial x_2)dx_2$ and $du_2(x_1, x_2) = (\partial u_2/\partial x_1)dx_1 + (\partial u_2/\partial x_2)dx_2$, which corresponds to four possible components for the mathematical representation of this deformation.

Taking Figure 4.6 of section 4.3.1 as a reference, the square denoted by ABCD is represented in Figure 4.11 as the unit area element in 2D considered at the point of coordinates x,y of edges dx and dy.

2) Provide an interpretation of the square in Figure 4.11 in the model used for the calculation of the strain tensor using Figure 4.6 as a reference.

Solutions:

A unit area element around point A_0 is considered in order to evaluate the strains of the material by determining how the vector **u(r)** is modified during a deformation. This is calculated from the derivatives of this vector with respect to coordinates by considering its modification at neighboring points B_0 and C_0 separated from A_0 by the distances dx_1 and dx_2, respectively. The square corresponds to the infinitesimal area in the surroundings of A_0 with its origin at A_0.

3) Provide an interpretation of the rhomboid in Figure 4.11 in the model used for the calculation of the strain tensor using Figure 4.6 as a reference.

Solutions:

When the material is deformed, at the point localized by **r** of components x_1, x_2 at A_0, and in its surroundings (B_0, C_0 and D_0), each component of **u(r)**, $u_1(x_1, x_2)$ and $u_2(x_1, x_2)$ is *a priori* subjected to different modifications depending on the position $x'_1 = x_1 + \alpha dx_1$ and $x'_2 = x_2 + \beta dx_2$ ($\alpha = 0$ or 1, $\beta = 0$ or 1). This different variation depending on the initial position A_0, B_0, C_0 or D_0, during the deformation, is represented on the figure by the vectors B_0B, C_0C and D_0D. The rhomboid is a schematic representation of the unit area deformed around point A separated from A_0 by $u(r)$.

4) What does the vector A_0A represent?

Solutions:

The vector A_0A in the figure is a translation vector $u(r)$ with its origin at A_0. Its components are $u_1(x_1, x_2)$ and $u_2(x_1, x_2)$.

5) What does the vector B_0B represent?

Solutions:

The vector B_0B in the figure is a translation vector $u(r+dr)$ with its origin at B_0. Its components are $u_1(x_1+d\,x_1, x_2)$ and $u_2(x_1+d\,x_1, x_2)$.

6) What does the vector C_0C represent?

Solutions:

The vector C_0C in the figure is a translation vector $u(r+dr)$ with its origin at C_0. Its components are $u_1(x_1, x_2+d\,x_2)$ and $u_2(x_1, x_2+d\,x_2)$.

7) Using the data in the figure, calculate tan α.

Solutions:

According to the figure, tan $\alpha = du_2(x_1, x_2)/(d\,x_1+du_1(x_1, x_2))$. Since $du_1(x_1, x_2)$ is small compared to $d\,x_1$ and for small angles, then $\alpha = du_2(x_1, x_2)/dx_1 = \partial u_2/\partial x_1$.

8) Using the data in the figure, calculate tan β.

Solutions:

According to the figure, tan $\beta = du_1(x_1, x_2) / (d\,x_2+du_2(x_1, x_2))$. Since $du_2(x_1, x_2)$ is small compared to $d\,x_2$ and for small angles, then $\beta = du_1(x_1, x_2)/dx_2 = \partial u_1/\partial x_2$.

9) $u_1(x_1+d\,x_1, x_2) - u_1(x_1, x_2)$ and give an interpretation of this result.

Solutions:

$$u_1(x_1+d\,x_1, x_2) - u_1(x_1, x_2) = du_1(x_1, x_2) = (\partial u_1/\partial x_1)dx_1.$$

This difference represents the elongation of the component u_1 of vector u parallel to OX_1. The elongation per unit length is the strain along OX_1.

10) $u_2(x_1+d\,x_1, x_2) - u_2(x_1, x_2)$ and give an interpretation of this result.

Solutions:

$u_2(x_1+d\,x_1, x_2)- u_2(x_1, x_2)= du_2(x_1, x_2)= (\partial u_2/\partial x_1)dx_1.$

This difference represents the elongation of the component u_2 of the vector u by rotation through an angle α. The elongation per unit length is the angle of rotation on the side dx_1.

11) $u_1(x_1, x_2+d\,x_2) - u_1(x_1, x_2)$ and give an interpretation of this result.

Solutions:

$u_1(x_1, x_2+d\,x_2)- u_1(x_1, x_2)= du_1(x_1, x_2)= (\partial u_1/\partial x_2)dx_2.$

This difference represents the elongation of the component u_1 of vector u by rotation with an angle β. The elongation per unit length is the angle of rotation on the side dx_2.

12) $u_2(x_1, x_2+d\,x_2) - u_2(x_1, x_2)$ and give an interpretation of this result.

Solutions:

$u_2(x_1, x_2+d\,x_2)- u_2(x_1, x_2)= du_2(x_1, x_2)= (\partial u_2/\partial x_2)dx_2.$

This difference represents the elongation of the component u_2 of vector u parallel to OX_2. The elongation per unit length is the strain along OX_2.

13) Calculate the components of the tensor based on elongations per unit length. Give the expressions of this tensor denoted by e_{ij}.

Solutions:

Given the calculations from 9 to 12, the following relations can be written:

$(\partial u_1/\partial x_1) = e_{11}$ and $(\partial u_2/\partial x_2)=e_{22}.$

Similarly: $(\partial u_1/\partial x_2) = e_{12}$ and $(\partial u_2/\partial x_1) = e_{21}$.

14) In the case of an overall rotation of the plane with an angle δ without strain, calculate the components of the tensor.

Solutions:

$e_{11}=e_{22}=0$ and $e_{12} = - e_{21} = \delta$ (as $\alpha >0$, but $\beta<0$).

15) Prove that the second rank tensor T_{ij} can be written in the form of a symmetric tensor S_{ij} and of an antisymmetric tensor A_{ij}.

Solutions:

Given $S_{ij}= (1/2(T_{ij}+T_{ji})$; it can be verified that $S_{ji} = S_{ij}$.

Given $A_{ij}= (1/2(T_{ij}-T_{ji})$; it can be verified that $A_{ji} = -A_{ij}$.

where $T_{ij} = S_{ij} +A_{ij}$.

16) Give the expressions of S_{ij} and A_{ij} in the case of tensor e_{ij}.

Solutions:

$S_{ij}= (1/2(e_{ij}+e_{ji})$ and $A_{ij}= (1/2(e_{ij}-e_{ji})$.

17) Provide an interpretation of the terms of S_{ij} and A_{ij}.

Solutions:

For an overall rotation: $S_{11}=S_{22}=0$ and $S_{12}= S_{21}=0$.

$A_{11}=A_{22}=0$ and $A_{12}= e_{12}$ and $A_{21}= -e_{21}$ (axial vector equivalent to a second rank antisymmetric tensor: a rotation axis and an angle about this axis).

In this case, the symmetric tensor S_{ij} represents the strain:

$S_{12}= (1/2(e_{12}+e_{21})$, $S_{21}= (1/2(e_{21}+e_{12})$ and $S_{11}= e_{11}$ and $S_{22}= e_{22}$.

As shown in questions (9) and (12), S_{11} and S_{22} represent an elongation strain or an expansion.

In this case, S_{12} and S_{21} represent a shear or a sliding strain (except for block rotation).

4.4.2. *A piezoelectric accelerometer*

In a piezoelectric accelerometer, a case (see Figure 4.12) is supported by a piezoelectric material that supplies an electric charge Q proportional to the corrective force, hence to the mass displacement. An accelerometer in longitudinal compression mode is considered, as illustrated in Figure 4.12. When the case is subjected to an acceleration a, a force of inertia F compresses the piezoelectric material in parallel to the direction of the acceleration which is labeled as axis 3. The dimensions at rest of a piezoelectric layer are t for the thickness, L for the length and W for the width. Its capacitance is denoted by C, and the corresponding dielectric permittivity is ε_{33}. The objective is to determine the static characteristics of the accelerometer.
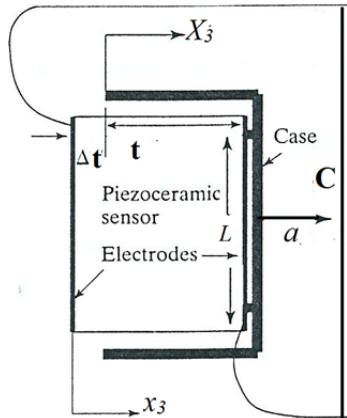

Figure 4.12. *Diagram of a piezoelectric accelerometer*

4.4.2.1.*Questions*

1) Find the vector expression of the strain tensor S of the layer.

2) The polarization of the layer being along the axis of deformation, find the vector expression of the polarization vector D of the layer.

3) Find the vector expression of the stress tensor T of the layer.

4) Relying on equations [4.63] and [4.64] expressed as $S = sT + dE$ and $D = dT + \varepsilon E$, deduce the equations verified by the piezoelectric layer for its mechanical strain and its electric polarization. (It is worth noting that there is no external electric stress, which means that $E = 0$.).

5) Based on the equations of question 4) show that: $\dfrac{Q}{\Delta t / t} = \dfrac{d_{33} L W}{s^E_{33}}$

6) Given: $t = 0.5$ mm; $L = 38.1$ mm; $W = 12.7$ mm; $\Delta t / t = 10^{-6}$; $d_{33} = 298.8 \ 10^{-12}$ CN-1; $s^E_{33} = 12.5 \ 10$ -12 $m^2 N^{-1}$; $\varepsilon_{33} = 11.95 \ 10^{-9}$ Fm^{-1}. Calculate: the charge Q, the capacitance C of the layer and the voltage V across the layer.

4.4.2.2. *Solutions*

1) Find the vector expression of the strain tensor S of the layer.

$$S = \begin{pmatrix} S_1 = & 0 \\ S_2 = & 0 \\ S_3 = & \Delta t / t \\ S_4 = & \\ S_5 = & \\ S_6 = & \end{pmatrix}$$

2) The polarization of the layer being along the axis of deformation, find the vector expression of the polarization vector D of the layer.

$$D = \begin{pmatrix} D_1 = & 0 \\ D_2 = & 0 \\ D_3 = & Q / LW \end{pmatrix}$$

3) Find the vector expression of the stress tensor T of the layer.

$$T = \begin{pmatrix} T_1 = & 0 \\ T_2 = & 0 \\ T_3 = & F/LW \\ T_4 = & 0 \\ T_5 = & 0 \\ T_6 = & 0 \end{pmatrix}$$

4) Relying on equations [4.63] and [4.64] expressed as $S = sT + dE$ And $D = dT + \varepsilon E$, deduce the equations verified by the piezoelectric layer for its mechanical strain and its electric polarization. (It is worth noting there is no external electric stress, which means that $E = 0$.)

1) $S_3 = s_{33}^E T_3 \Rightarrow \dfrac{\Delta t}{t} = s_{33}^E \dfrac{F}{LW}$ and 2) $D_3 = d_{33} T_3 \Rightarrow \dfrac{Q}{LW} = d_{33} \dfrac{F}{LW}$

5) Based on the equations of question 4 show that: $\dfrac{Q}{\Delta t/t} = \dfrac{d_{33} LW}{s_{33}^E}$

Equations 1 and 2 from the previous solution lead to:

$$\dfrac{\dfrac{Q}{LW}}{\dfrac{\Delta t}{t}} = \dfrac{d_{33} \dfrac{F}{LW}}{s_{33}^E \dfrac{F}{LW}} \Rightarrow \dfrac{Q}{\dfrac{\Delta t}{t}} = \dfrac{d_{33} LW}{s_{33}^E}$$

6) Given: $t = 0.5$ mm; $L = 38.1$ mm; $W = 12.7$ mm; $\Delta t/t = 10^{-6}$; $d_{33} = 298.8 \ 10^{-12} \ CN^{-1}$; $s_{33}^E = 12.5 \ 10^{-12} \ m^2 N^{-1}$; $\varepsilon_{33} = 11.95 \ 10^{-9} \ Fm^{-1}$. Calculate: the charge Q, the capacitance C of the layer and the voltage V across the layer.

$$Q = \dfrac{\Delta t}{t} \bigg/ \dfrac{d_{33} LW}{s_{33}^E} \qquad \text{AN : Q} = 1{,}1157 \ 10^{-8} \ C$$

$$C = \dfrac{\varepsilon \times \text{surface}}{\text{distance}} \Rightarrow C = \dfrac{\varepsilon_{33} \times LW}{t} \qquad \text{A.N. C} = 1{,}156 \ 10^{-8} \ F$$

$Q = CV \Rightarrow V = Q/C = 1$ V.

4.4.3. *Piezoelectric transducer*

Piezoelectric materials can be stacked in the form of layers either mechanically in series or electrically in parallel as shown in Figure 4.13.
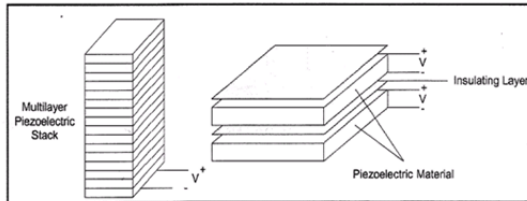

Figure 4.13. *Diagram of a piezoelectric transducer*

The stack on the right of this figure is considered for this exercise. Equations [4.63] and [4.64] are expressed as $S=sT+dE$ and $D=dT+\varepsilon E$, respectively. The objective is to determine the force, the displacement and the capacitance as a function of external excitations in the absence of stress and strain. The following conventions are adopted for the usual axes Ox, Oy and Oz by denoting them as 1, 2 and 3, respectively, as shown in Figure 4.14 and the stresses and strains are all considered zero, except for S_3 and T_3, respectively. Similarly, the electric field and the electric displacement are parallel to axis 3, which means that $E_1 = E_2 = 0$ and $D_1 = D_2 = 0$.
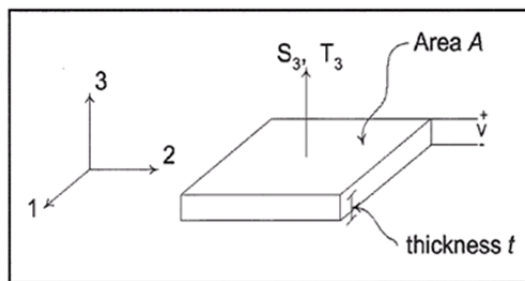

Figure 4.14. *Piezoelectric layer*

4.4.3.1. *Questions*

1) Express S_3 and D_3 as a function of T_3 and E_3. $x_i = \int_0^t S_3 dx_3$

2) The elongation of the ith layer is given by:

Deduce x_i as a function of s_{33}, d_{33}, T_3 and E_3.

3) Express E_3 and T_3 as a function of the given data.

4) Deduce from question 3, the final expression of x_i.

5) Assume that the transducer is composed of n layers and that the total length of the transducer is L. What is its total elongation X in this case?

6) The amount of charges due to the ith layer is given by:

$$q_i = \iint_{surface} D_3 dx_1 dx_2$$

Deduce from this expression, q_i as a function of d_{33}, ε_{33}, T_3 and E_3. Then express the total charge Q on the faces of the transducer as a function of d_{33}, L, t, F, n, A, V and ε_{33}.

7) Express the relation between X and Q and F and V in matrix form. Give an interpretation of the various elements of this 2 x 2 matrix.

8) Consider the situation of a zero force or of a zero strain on the transducer as shown in Figure 4.15(a) and (b).

Find in each case the expression of the force and of the displacement of the transducer and of the charge.

9) Deduce from results of question 8) that the capacitance C can be expressed in the following form: $(1 - k_{33}^2) (n\varepsilon_{33}A) /t$. Find in each case the expression of k_{33}^2.

10) Calculate the stress for an electric field of 0.5 MV/m and a strain of 10 MPa applied to the piezoelectric material. The inverse of Young's modulus is, $1/Y = s = 20 \ 10^{-12}$ m²/N and the piezoelectric stress coefficient is $d_{33} = 650 \ 10^{-12}$ m/V.

11) Find the geometry of a stack of piezoelectric layers subjected to a blocking force of 1000 N and a free displacement of 30 μm. The inverse of Young's modulus is, $1/Y = s = 20 \ 10^{-12}$ m²/N, the piezoelectric stress

coefficient is $d_{33} = 650 \ 10^{-12}$ m/V, the layer thickness is 254 μm, and the maximum allowed electric field is 0.3 MV/m.
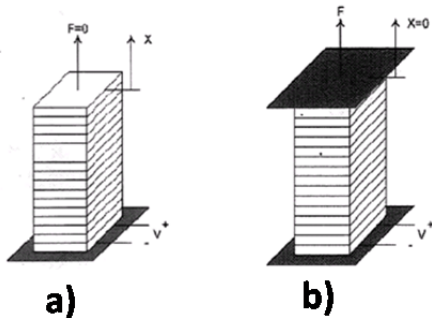
**Figure 4.15.** *a) Zero forces and b) zero strain*

4.4.3.2. *Solutions*

1) Express S_3 and D_3 as a function of T_3 and E_3.

From

$$\underline{S} = s\underline{T} + d\underline{E}$$
$$\underline{D} = d\underline{T} + \varepsilon\underline{E}$$

It can be deduced that:

$$S_3 = S_{33}^E T_3 + d_{33}E \text{ and } D_3 + d_{33}T_3 + \varepsilon_{33}^T E$$

2) The elongation of the ith layer is given by: $x_i = \int_0^t S_3 dx_3$. Deduce x_i as a function of s_{33}, d_{33}, T_3 and E_3.

For the ith layer: $x_i = \int_0^t (s_{33}^E T_3 + d_{33}E_3)dx_3 = (s_{33}^E T_3 + d_{33}E_3)t$

3) Express E_3 and T_3 as a function of the given data:

$$E_3 = \frac{V}{t} \text{ and } T_3 = \frac{F}{A}$$

If there are no stress and strain, then:

4) Deduce the final expression of x_i

Result:

$$x_i = s_{33}^E \frac{F}{A} t + d_{33} \frac{V}{t} t = s_{33}^E \frac{F}{A} t + d_{33}V$$

5) Assume that the transducer is composed of n layers and that the total length of the transducer is L. What is its total elongation X in this case?

Result:

$$X = \sum_i x_i = nx_i = \frac{L}{t}(s_{33}^E \frac{F}{A} t + d_{33}V) = s_{33}^E \frac{FL}{A} + d_{33}V \frac{L}{t}$$

6) The amount of charges due to the ith layer is given by:

$$q_i = \iint_{surface} D_3 dx_1 dx_2$$

Deduce from this expression, q_i as a function of d_{33}, ε_{33}, T_3 and E_3. Then express the total charge Q on the faces of the transducer as a function of d_{33}, L, t, F, n, A, V and ε_{33}.

Result:

$$q_i = \iint_S (d_{33}T_3 + \varepsilon_{33}^T E_3) dx_1 dx_2 = d_{33}T_3 A + \varepsilon_{33}^T E_3 A$$

Hence:

$$Q = \sum_i q_i = nq_i = \frac{L}{t} d_{33} \frac{F}{A} A + \frac{L}{t} \varepsilon_{33}^T \frac{V}{t} A = \frac{L}{t} d_{33}F + \varepsilon_{33}^T n \frac{V}{t} A$$

7) Express the relation between X and Q and F and V in matrix form. Give an interpretation of the various elements of this 2 x 2 matrix.

$$X = \frac{S_{33}^E L}{A} F + \frac{d_{33}L}{t} V \text{ and } Q = \frac{d_{33}L}{t} F + \frac{\varepsilon_{33}^T nA}{t} V$$

It can be written that:

Hence, the matrix form: $\begin{pmatrix} X \\ Q \end{pmatrix} = \begin{pmatrix} \dfrac{s_{33}^{E}L}{A} & \dfrac{d_{33}L}{t} \\ \dfrac{d_{33}L}{t} & \dfrac{\varepsilon_{33}^{T}nA}{t} \end{pmatrix} \begin{pmatrix} F \\ V \end{pmatrix}$

The various terms can be interpreted as follows:

The first term (M_{11}) is the displacement under the effect of the mechanical force in the absence of electric stress (or electric field): it is the compliance or the mechanical elasticity coefficient or the inverse Young's modulus ($X=CF$ or $F=YX$)) (m/N).

The second term (M_{12}) is the displacement under the effect of the electric stress (or electric field): it is the piezoelectric coupling coefficient (m/V).

The third term (M_{21}) corresponds to the appearance of electric charges under the effect of a mechanical force in the absence of electric stress (or electric field): it is the piezoelectric coupling coefficient (m/V).

The fourth term (M_{22}) is the displacement under the effect of electric constraint (or electric field): it is the capacitance ($Q=CV$; C in Farads).

8) Consider the situation of a zero force or of a zero strain on the transducer as shown in Figure 4.15(a) and (b).

Find in each case the expression of the force and of the displacement of the transducer and of the charge.

a) Zero force: $F= X = \dfrac{d_{33}L}{t}V = nd_{33}V$ and $\qquad Q = \dfrac{\varepsilon_{33}^{T}nA}{t}V = C^{T}V$

b) Zero strain, X=0: $0 = \dfrac{s_{33}^{E}L}{A}F + \dfrac{d_{33}L}{t}V \Rightarrow F = -\dfrac{d_{33}A}{s_{33}^{E}t}V$

and $Q = \dfrac{d_{33}L}{t}F + \dfrac{\varepsilon_{33}^{T}nA}{t}V = -\dfrac{d_{33}^{2}AL}{s_{33}^{E}t^{2}}V + \dfrac{\varepsilon_{33}^{T}nA}{t}V = (-\dfrac{d_{33}^{2}}{s_{33}^{E}} + \varepsilon_{33}^{T})\dfrac{nA}{t}V$

9) Deduce from the results of question 8 that the capacitance C can be expressed in the following form: $(1 - k_{33}{}^{2})\,(n\varepsilon_{33}A)\,/t$. Find in each case the expression of $k_{33}{}^{2}$.

a) $k_{33}^2 = 0$

b) $Q = CV \Rightarrow C = (-\frac{d_{33}^2}{s_{33}^E} + \varepsilon_{33}^T)\frac{nA}{t} = (1 - \frac{d_{33}^2}{\varepsilon_{33}^T s_{33}^E})\frac{nA\varepsilon_{33}^T}{t} = (1 - k_{33}^2)C^T$

10) Calculate the stress for an electric field of 0.5 *MV/m* and a strain of 10 *MPa* applied to the piezoelectric material. The inverse of Young's modulus is, $1/Y = s = 20 \times 10^{-12}$ *m²/N*, and the piezoelectric stress coefficient is $d_{33} = 650 \times 10^{-12}$ *m/V*.

$$\frac{X}{L} = s_{33}^E \frac{F}{A} + d_{33} \frac{V}{t} \Rightarrow S = s_{33}^E T + d_{33} E$$

Hence: $S = (20 \ 10^{-12} \times 10 \ 10^6) + (650 \ 10^{-12} \times 0.5 \ 10^6) = 525 \times 10^{-6}$.

11) Find the geometry of a stack of piezoelectric layers subjected to a blocking force of 1000 *N* and a free displacement of 30 μm. The inverse of Young's modulus is, $1/Y = s = 20 \times 10^{-12}$ *m²/N*, the piezoelectric stress coefficient is $d_{33} = 650 \times 10^{-12}$ *m/V*, the layer thickness is 254 μm, and the maximum allowed electric field is 0.3 *MV/m*.

The free displacement is: $\frac{X}{L} = d_{33}\frac{V}{t} \Rightarrow L = \frac{X}{d_{33}E}$

Hence: $L = (30 \times 10^{-6} / (650 \times 10^{-12} \times 0.3 \times 10^6) = 0.154$ m.

The blocking force is: $F = -\frac{d_{33}A}{s_{33}^E t}V = -\frac{d_{33}A}{s_{33}^E}E \Rightarrow A = \left|\frac{Fs_{33}^E}{d_{33}E}\right|$

Hence: $A = (1000 \times 20 \times 10^{-12)} / (650 \ 10^{-12} \times 0.3 \times 10^6) = 1.03 \times 10^{-4}$ m².

The calculated number of layers is: $n = L/t = (0.154/254 \times 10^{-6}) = 607$.

4.4.4. *Piezoelectric sensor*

Piezoelectric materials can be stacked as double layers (see Figure 4.16(a)) that constitute a force sensor as in a scanning probe microscope used for studying the topography of nanomaterial surfaces.

The objective is to determine the force, the displacement and the capacitance as a function of external excitations in the absence of stress and strain. Equations [4.63] and [4.64] are expressed as $S=sT+dE$ and $D=dT+\varepsilon E$, respectively. By convention, the Ox, Oy and Oz axes are denoted by 1, 2 and

3, respectively, as shown in Figure 4.16(b), and all the stresses and strains are considered to be zero, except for S_1 and T_1, respectively. Similarly, the electric field and the electric displacement are parallel to axis 3, meaning that $E_1 = E_2 = 0$ and $D_1 = D_2 = 0$.


a)   b)
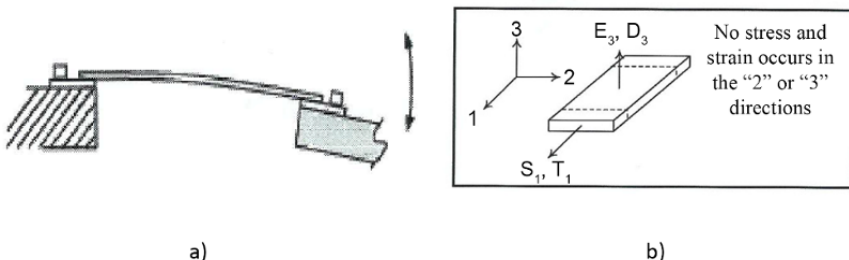
Figure 4.16. *a) Piezoelectric sensor and b) piezoelectric layer*

4.4.4.1. *Questions*

1) Based on the following general constitutive equations of a piezoelectric material: $\begin{aligned} \underline{S} &= s\underline{T} + d\underline{E} \\ \underline{D} &= d\underline{T} + \varepsilon\underline{E} \end{aligned}$ express S_1 and D_3 as a function of T_1 and E_3.

Consider the stack shown in Figure 4.17 and the associated electric circuit such that the top and bottom layers are subjected to an electric field whose direction is, respectively, parallel and antiparallel to the direction of the layer polarization. It is assumed that $L \gg t$.
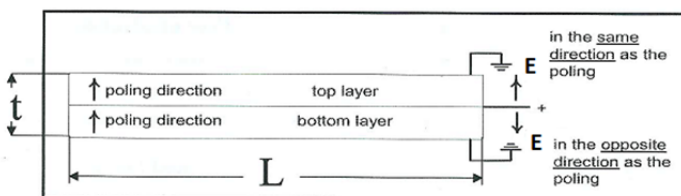
Figure 4.17. *Piezoelectric double layer*

2) Consider that the stress T is zero. Calculate S_1 for each layer. Compare the sign and comment the diagrams in Figure 4.18(a) and (b).
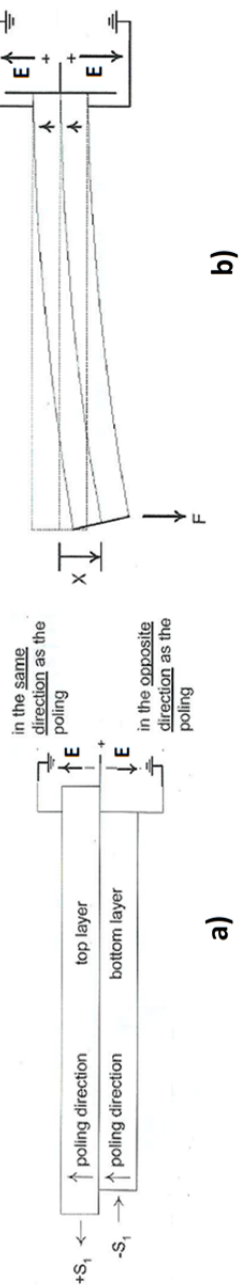
Figure 4.18. *a) Piezoelectric double layer and b) bending of layers*

The bending of the layer is parameterized by the X variable, which gives the vertical displacement of the contact plane between the two layers.

Given: $X = 4 \dfrac{s_{11}^E L^3}{wt^3} F + 3 \dfrac{d_{31} L^2}{t^2} V$

3) What is the free displacement X of the two layers ($F=0$)?

4) Calculate the force F required to cancel the displacement X ($X=0$).

5) What is the effect of the ratio L/t on X and F calculated in solutions 3 and 4?

4.4.4.2. *Solutions*

1) Based on the following general constitutive equations of a piezoelectric material: $\begin{aligned} \underline{S} &= s\underline{T} + d\underline{E} \\ \underline{D} &= d\underline{T} + \varepsilon\underline{E} \end{aligned}$ express S_1 and D_3 as a function of T_1 and E_3.

Based on the general equation and since only T_1, S_1, E_3 and D_3 are different from zero, the relations can be written as follows:

$$S_1 = s_{11}^E T_1 + d_{13} E_3$$
$$D_3 = d_{31} T_1 + \varepsilon_{33}^T E_3$$

2) Consider that the stress T is zero. Calculate S_1 for each layer. Compare the sign and comment the diagrams in Figure 4.18(a) and (b).

In the absence of stress T, equation 1 of the first question, for the top and bottom layers, leads, respectively, to:

$$S_1 = +d_{13} E_3$$
$$S_1 = -d_{13} E_3$$

Comparison: the signs are opposite, as the electric potential difference is in opposition.

Comments: an expansion of the top layer and a contraction of the bottom layer can be noted in Figure 4.18(a), which is in agreement with the results of the calculations. The bending of the double layer minimizes the stresses and prevents the fracture of the two layers.

3) What is the free displacement X of the two layers ($F=0$)?

The calculation leads to:

$$X = 3\frac{d_{31}L^2}{t^2}V$$

4) Calculate the force F required for cancelling out the displacement X ($X=0$).

The calculation yields:

$$F = -\frac{(3\frac{d_{31}L^2}{t^2}V)}{(4\frac{s_{11}^E L^3}{wt^3})} = -(\frac{d_{31}wt}{s_{11}^E L})V$$

5) What is the effect of the ratio L/t on X and F calculated in solutions 3 and 4?

X depends on L/t while F is inversely proportional to L/t. Increasing L/t leads to an increase of X and a decrease of the force, F.

4.5. Appendix: crystal symmetry

In condensed phase, only the rotation axes of orders 1, 2, 3, 4 and 6 enable a periodic pavement of the space compatible with crystalline lattices. The symmetry elements used by the crystallographers to define the symmetry about a point in space, for example, the central point of the unit cell, are: a point (center) of symmetry, rotation axes, mirror planes, and combinations thereof. Using these elements of symmetry, it is shown in crystallography that there are 32 symmetry point groups (Table 4.8) based on symmetry operations. The various symmetry elements are divided into

seven crystalline systems as follows: triclinic, monoclinic, orthorhombic, tetragonal, rhombohedral, hexagonal and cubic.

Crystalline system	Number of point groups	Herman-Mauguin	Schoenflies
Triclinic	2	$1, \bar{1}$	C_1, C_i
Monoclinic	3	$2, m, 2/m$	C_2, C_s, C_{2h}
Orthorhombic	3	$222, 2mm, mmm$	$D_2, C_{2v}, D_{2h},$
Rhombohedral	5	$3, 32, 3m$ $\bar{3}, \bar{3}m$	C_3, D_3, C_{3v} S_6, D_{3d}
Hexagonal	7	$6, 622, 6mm, 6/m,$ $\bar{6}, \bar{6}2m, 6/mmm$	C_6, D_6, C_{6v}, C_{6h} C_{3h}, D_{3h}, D_{6h}
Tetragonal (quadratic)	7	$4, \bar{4}, 422, 4mm,$ $\bar{4}2m, 4/m, 4/mmm$	$C_4, S_4, D_4, C_{4v},$ D_{2d}, C_{4h}, D_{4h}
Cubic	5	$23, m3, 432,$ $\bar{4}3m, m3m$	T, T_h, O T_d, O_h

Table 4.8. *The point groups of 32 classes of symmetry and the equivalence between Schoenflies and Hermann–Mauguin symbols*

There are special point groups that can be added to the above groups. Among them, the continuous point groups have an infinite number of symmetry elements, the axial and spherical groups of symmetry used for listing the groups characterized by the presence of several rotational symmetry axes of high order n associated with regular polyhedrons, Platonic solids, such as the triangular tetrahedron, the cube with six square faces, the octahedron with eight triangular faces, the dodecahedron with 12 regular pentagonal faces with three pentagonal faces joined at one point and the icosahedron with 20 equilateral triangular faces with five faces joined at one point.

Table 4.9 summarizes the two conventions used to represent a symmetry element in a crystal.

Symmetry operation	Herman-Mauguin	Schoenflies
Identity	1	C_1 or E
Rotation ($2\pi/n$)	n	C_n
Mirror	m	σ, C_s, S_1
Inversion	$\bar{1}$	i, C_i, S_2
Rotation-Reflection	-	S_{2n}
Rotation-Inverison	$\bar{n}$	-

Table 4.9. *Schoenflies and Hermann–Mauguin notation*

The convention used in condensed phase is that of Hermann–Mauguin, which is preferred in crystallography to that of Schoenflies which is used in the spectroscopy study of atoms and molecules: the cyclic groups are denoted by their order n (rotational axis of symmetry of order n), a plane of symmetry is denoted by m and the group is denoted by nm ($C_{2v} \equiv 2m$); if the plane is perpendicular to the axis of symmetry, n/m ($C_{2h} \equiv 2/m$) is used; the presence of a center of symmetry is indicated by a bar above the order of the group ($C_i = S_2 \equiv \bar{1}$, $S_4 \equiv \bar{4}$, $S_6 = C_i \otimes C_3 \equiv \bar{3}$). For example, $O_h \equiv m3m$ and $D_{3h} \equiv \bar{3}m2$, etc.

Appendix

Propagation of a Light Ray

In light diffraction problems, the amplitude of a wave $E_z(x,y)$ on a surface located in a plane z is determined by the amplitude $E_0(x,y)$ of a wave in the plane $z = 0$.

In Chapter 3 of [DAH 16], equation 3.6 gives the expression of an electromagnetic wave traveling along Oz, in the form $u(z-vt)=acos(k(z-ct))$, where v is the speed of propagation of the wave in a medium of index n, a is its amplitude and $k=2\pi n/\lambda$. In a vacuum, $n=1$ and in a three-dimensional space the monochromatic plane wave of the angular frequency $\omega=kc$ and the wave vector $k = (k_x, k_y, k_z)$ can be expressed in the form $E = E_0 \; exp \; i(2\pi/\lambda (\alpha x+\beta y+\gamma z) - \omega t)$, where the components of the wave vector have the form: $k_x=2\pi\alpha/\lambda$, $k_y=2\pi\beta/\lambda$ and $k_x=2\pi\gamma/\lambda$, with α, β, γ being the direction cosines of the wave vector **k** and λ being the wavelength. This expression can be obtained by solving the Helmholtz equation (equation 3.7, [DAH 16]):

$$\Delta \vec{E} + \frac{\omega^2}{c^2}\vec{E} = \vec{0} \qquad\qquad [A.1]$$

where $\Delta\vec{E} = \vec{\nabla}^2\vec{E}$, using Green's function $G_k(\vec{r},\vec{r}_0)$ of the Helmholtz equation that verifies that:

$$(\nabla^2 + k^2)G_k(\vec{r},\vec{r}_0) = \delta(\vec{r} - \vec{r}_0) \qquad\qquad [A.2]$$

given that $G_k(\vec{r},\vec{r}_0) = -\frac{exp(ik|\vec{r}-\vec{r}_0|)}{4\pi|\vec{r}-\vec{r}_0|}$, where the unit vector is $\vec{e}_r = \frac{(\vec{r}-\vec{r}_0)}{|\vec{r}-\vec{r}_0|}$. The solution is readily obtained, since for the k mode of the electric field generated by a source placed at $\vec{r}_0$, $\vec{E}_k(\vec{r},\vec{r}_0) = -\frac{exp(ik|\vec{r}-\vec{r}_0|)}{4\pi|\vec{r}-\vec{r}_0|}\vec{e}_r$.

The propagation of a wave through obstacles (slits or opaque objects) can be determined using the Green–Ostrogradsky theorem and the Green function $G_k(\vec{r}, \vec{r}_0)$ of the Helmholtz equation.

Based on the relation:

$$\vec{\nabla}(u\vec{\nabla}v - v\vec{\nabla}u) = u\vec{\nabla}^2 v - v\vec{\nabla}^2 u = u\Delta v - v\Delta u \qquad [A.3]$$

where u and v are solutions to the Helmholtz equation and the Green–Ostrogradsky theorem, which enables a volume integral to be transformed into a surface integral:

$$\int (u\Delta v - v\Delta u)d\tau = \int (u\vec{\nabla}^2 v - v\nabla^2 u)d\tau = \oint (u\vec{\nabla}v - v\vec{\nabla}u)d\vec{s} \quad [A.4]$$

It can be written that:

$$\int \left(\vec{E}(\vec{r})\Delta G_k(\vec{r}, \vec{r}_0) - G_k(\vec{r}, \vec{r}_0)\Delta\vec{E}(\vec{r}) \right) d\tau = \int \vec{E}(\vec{r})\delta(\vec{r} - \vec{r}_0)d\tau$$

$$- \int \vec{E}(\vec{r})k^2 G_k(\vec{r}, \vec{r}_0)d\tau + \int G_k(\vec{r}, \vec{r}_0)k^2\vec{E}(\vec{r})d\tau = \vec{E}(\vec{r}_0) \qquad [A.5]$$

hence

$$\vec{E}(\vec{r}_0) = \oint \left(\vec{E}(\vec{r})\vec{\nabla}G_k(\vec{r}, \vec{r}_0) - G_k(\vec{r}, \vec{r}_0)\vec{\nabla}\vec{E}(\vec{r}) \right) d\vec{s}$$

$$= \oint (\vec{E}(\vec{r})\{\vec{\nabla}G_k(\vec{r}, \vec{r}_0)d\vec{s} - ikG_k(\vec{r}, \vec{r}_0)ds\}) \qquad [A.6]$$

where the surface integral surrounds the point located at $\vec{r}_0$ and $\vec{r}$ indicates the position of the surface element $d\vec{s}$, (Figure A.1) so that $\vec{\nabla}\vec{E}(\vec{r}).d\vec{s} = ik\vec{E}(\vec{r})ds$, for a wave that propagates in the volume surrounded by an integration surface ds. For a wave that propagates outside the surface, the relation is $\vec{\nabla}\vec{E}(\vec{r}).d\vec{s} = -ik\vec{E}(\vec{r})ds$.

Given that $G_k(\vec{r}, \vec{r}_0) = -\dfrac{exp(ik|\vec{r}-\vec{r}_0|)}{4\pi|\vec{r}-\vec{r}_0|}$, then:

$$\vec{\nabla}G_k(\vec{r}, \vec{r}_0) = ikG(\vec{r}, \vec{r}_0)\vec{e}_r + \frac{exp(ik|\vec{r} - \vec{r}_0|)}{4\pi|\vec{r} - \vec{r}_0|^2}\vec{e}_r$$

$$= \left(\frac{ik}{|\vec{r}-\vec{r}_0|} - \frac{1}{|\vec{r}-\vec{r}_0|^2} \right)(\vec{r} - \vec{r}_0)G_k(\vec{r}, \vec{r}_0) \qquad [A.7]$$
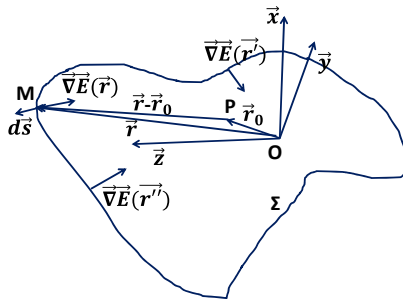
Figure A.1. *Kirchhoff's integral over a surface Σ passing through a point M surrounding point P. For a color version of this figure, see www.iste.co.uk/dahoo/metrology1.zip*

At a large distance compared to the wavelength such that $k|\vec{r} - \vec{r}_0| \gg 1$, the solution is:

$$\vec{E}(\vec{r}_0) = \oint \left(\vec{E}(\vec{r}) \left\{ \frac{ik}{|\vec{r}-\vec{r}_0|} (\vec{r} - \vec{r}_0) G_k(\vec{r}, \vec{r}_0) d\vec{s} - ik G_k(\vec{r}, \vec{r}_0) ds \right\} \right) \quad [A.8]$$

or:

$$\vec{E}(\vec{r}_0) = -\frac{ik}{4\pi} \oint \vec{E}(\vec{r}) \frac{exp(ik|\vec{r}-\vec{r}_0|)}{|\vec{r}-\vec{r}_0|^2} \left((\vec{r} - \vec{r}_0) d\vec{s} - |\vec{r} - \vec{r}_0| ds \right) \quad [A.9]$$

This solution corresponds to the formulation of the Huygens–Fresnel principle or the Huygens–Fresnel equation obtained using Kirchhoff's integral, which is the Fresnel–Kirchhoff diffraction formula.

When a monochromatic plane wave traveling in parallel to Oz meets a screen (E_0) with a slit (Figure A.2), a diffraction pattern appears in the observation plane. For the sake of simplicity, assume that the slit plane is perpendicular to the direction of propagation of the plane wave and that the amplitude and the gradient of the electric field of the wave are constant on the surface of the slit in the vicinity of M (Figure A.2) and zero everywhere else. The amplitude on the other side of the slit at a point P located at $\vec{r}_0$ is given by the Fresnel–Kirchhoff diffraction formula. If the slit is in the Oxy plane (Figure A.2), and the dimensions are small compared to the position of point P at $\vec{r}_0$, the amplitude of the field at P is given by:

$$\vec{E}(\vec{r}_0) = -\frac{ik\vec{E}(\vec{r})}{4\pi R} (cos\theta + 1) \oint exp(ik|\vec{r} - \vec{r}_0|) dx dy \quad [A.10]$$

where R is the distance between the central point of the slit and point P (in a first approximation, it is the same distance for all the points of the slit), and θ is the angle between the Oz axis and the vector $\vec{MP} = \vec{r}_0 - \vec{r}$. The origin of coordinates is considered in the plane containing the diffraction slit.
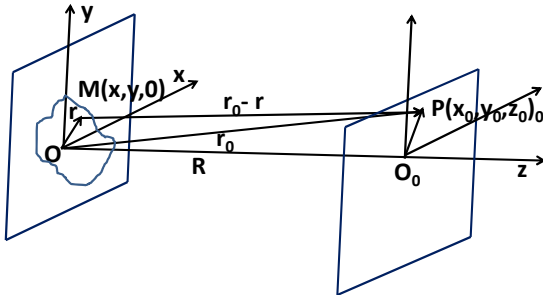
Figure A.2. *Diagram of diffraction in a plane containing P through a slit containing M. For a color version of this figure, see www.iste.co.uk/dahoo/metrology1.zip*

The module of the vector $\vec{r}_0 - \vec{r}$ is given by:

$$|\vec{r}_0 - \vec{r}| = \sqrt{r_0^2 - 2\vec{r}_0.\vec{r} + r^2}.$$

Considering the conditions of Fraunhofer diffraction in the far field, with an origin O in the slit plane (Figure A.2), where R is the distance between the observation plane and the diffraction plane, the following relation can be obtained:

$$exp(ik|\vec{r} - \vec{r}_0|) = exp\left(ik\sqrt{r_0^2 - 2\vec{r}_0.\vec{r} + r^2}\right) =$$
$$e^{ikR}exp\left(-ik(\alpha x + \beta y)\right) \tag{A.11}$$

where: $\alpha = \frac{x_0}{R}$ and $\beta = \frac{y_0}{R}$.

According to the Gaussian approximation of paraxial rays, the field at P is:

$$\vec{E}(\vec{r}_0) = A \oiint exp\left(-ik(\alpha x + \beta y)\right)dxdy \tag{A.12}$$

Fraunhofer diffraction at large distance can be calculated using this formula. For a circular hole, the formula is:

$$\vec{E}(\vec{r}_0) = A \oiint exp\left(-ik(\alpha\rho cos\varphi)\right)\rho d\rho d\varphi$$

$$= 2\pi A \int_0^a J_0(k\alpha\rho)\rho d\rho = 2\pi A a^2 \frac{J_1(k\alpha\rho)}{k\alpha\rho} \qquad \text{[A.13]}$$

where $J_0(x)$ and $J_1(x)$ are zero and the first-order Bessel functions.
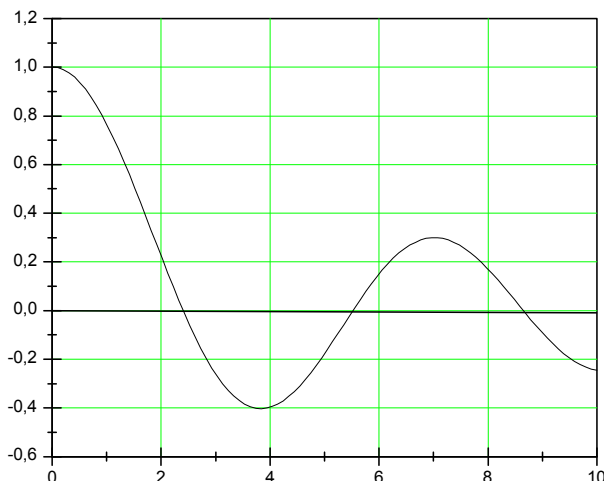
Figure A.3. *Distribution of the diffraction amplitude through a circular hole. For a color version of this figure, see www.iste.co.uk/dahoo/metrology1.zip*

Fresnel diffraction is obtained for an observation plane that is closer to the slit. In this case, second-order terms in x should be considered. Moreover, it is wise to use a coordinate system so as to get rid of the terms of order 1 in x and y. Assume that the slit is in the Oxy plane and the Oz axis is a line perpendicular to the plane that passes through the point of observation r_0. In this system of coordinates, $\alpha = \beta = \vec{r}.\vec{r}_0 = 0$. Under these conditions, the following expression is obtained:

$$exp(ik|\vec{r} - \vec{r}_0|) = exp\left(ik\sqrt{r_0^2 - 2\vec{r}_0.\vec{r} + r^2}\right) = e^{ikR} exp\left(\frac{ik(x^2+y^2)}{2R}\right) \text{[A.14]}$$

In the case of the Gaussian approximation of paraxial rays, the field at P is given by:

$$\vec{E}(\vec{r}_0) = A \int exp \left(\frac{ikx^2}{2R} \right) dx \int exp \left(\frac{iky^2}{2R} \right) dy \qquad \text{[A.15]}$$

which can be used to calculate the Fresnel diffraction pattern.

References

[ABB 73] ABBE E., "Beiträge zur theorie des mikroskops und der mikroskopischen wahrnehmung", *Arch. Mikroskop. Anat.*, vol. 9, pp. 413–418, 1873.

[ASH 72] ASH E.A., NICHOLLS G., "Super-resolution aperture scanning microscope", *Nature*, vol. 237, p. 510A, 1972.

[ASP 82] ASPECT A., DALIBARD J., ROGER G., "Experimental test of Bell's inequalities using time varying analyzers", *Phys. Rev. Lett.*, vol. 49, no. 25, pp. 1804–1807, 1982.

[BAR 48] BARDEEN J., BRATTAIN W.H., "The transistor, a semi-conductor triode", *Phys. Rev.*, no. 74, pp. 230–231, 1948.

[BET 86] BETZIG E., LEWIS A., HAROOTUNIAN A. *et al.*, "Near-field scanning optical microscopy (NSOM); development and biophysical applications", *Biophys. J.*, vol. 49, pp. 269–279, 1986.

[BET 87] BETZIG E., ISAACSON M., LEWIS A., "Collection mode near-field optical microscopy", *Appl. Phys. Lett.*, vol. 51, pp. 2088–2090, 1987.

[BIN 82a] BINNIG G., ROHER H., GERBER C. *et al.*, "Tunneling through a controllable vacuum gap", *Appl. Phys. Lett.*, vol. 40, pp. 178–180, 1982.

[BIN 82b] BINNIG G., ROHER H., "Scanning tunneling microscopy", *Helv. Phys. Acta*, vol. 55, pp. 726–735, 1982.

[BIN 83] BINNIG G., ROHER H., "Scanning tunneling microscopy", *Surf. Sci.*, vol. 126, pp. 236–244, 1983.

[BIN 86a] BINNIG G., ROHRER H. "Scanning tunneling microscopy", *IBM J. Res. Dev.*, vol. 30, pp. 355–369, 1986.

[BIN 86b] BINNIG G., QUATE C.F., GERBER C., "Atomic force microscope", *Phys. Rev. Lett.*, vol. 56, pp. 930–933, 1986.

[BIO 56] BIOT M.A., "Thermoelasticity and irreversible thermodynamics", *J. Appl. Phys.*, vol. 27, pp. 240–253, 1956.

[BRA 78] BRACEWELL R., *The Fourier Transform and its Applications*, McGraw-Hill Book Co., 1978.

[BRI 38] BRILLOUIN L., *Les tenseurs en mécanique et en élasticité*, Editions Masson et Cie, Paris, 1938.

[BRO 68] BROGLIE DE L., *Ondes électromagnétiques et photons*, Gauthier-Villars, Paris, 1968.

[BRU 55] BRUHAT G., *Mécanique*, Editions Masson et Cie., Paris, 1955.

[BRU 62] BRUHAT G., *Thermodynamique*, Editions Masson et Cie., Paris, 1962.

[BRU 65] BRUHAT G., *Cours de physique générale optique*, Editions Masson et Cie, Paris, 1965.

[COA 12] COANGA J.M., ALAYLI N., DAHOO P.R., "Metrological applications of ellipsometry with temperature change", *Proceedings of 4th International Metrology Conference 23–27 April 2012 (CAFMET 2012) Marrakech, Morocco*, Curran Associates, Inc., July 2012.

[COH 73] COHEN-TANNOUDJI C., DIU B., LALOE F., *Mécanique quantique*, Herman, Paris, 1973.

[COL 72] COLELLA R., MENADUE J.F., "Comparison of experimental and beam calculated intensities for glancing incidence high-energy electron diffraction", *Acta Cryst.*, vol. A28, pp. 16–22, 1972.

[COU 89] COURJON D., SARAYEDDINE K., SPAJER M., "Scanning tunneling optical microscopy", *Opt. Comm.*, vol. 71, pp. 23–281, August 2, 1989.

[CUR 80] CURIE J., CURIE P., "Développement, par pression, de l'électricité polaire dans les cristaux hémièdres à faces inclinées", *Comptes rendus de l'Académie des Sciences*, vol. XCI, pp. 294–295, August 2, 1980.

[CUR 81] CURIE P., CURIE J., "Contractions et dilatations produites par des tensions électriques dans les cristaux hémièdres à faces inclinées", *Comptes rendus de l'Académie des Sciences*, vol. XCIII, pp. 1137–1140, December 26, 1981.

[DAH 99] DAHOO P.R., BERRODIER I., RADUCU V. *et al*., "Splitting of ν_2 vibrational mode of CO_2 isotopic species in the unstable trapping site in argon matrix", *Eur. Phys. J. D*, vol. 5, pp. 71–81, 1999.

[DAH 03] DAHOO P.R., HAMON T., SCHNEIDER M. *et al.*, "Ellipsometry: Principles, signal processing and applications to metrology", *Proceedings CIMNA*, Lebanon, 2003.

[DAH 04a] DAHOO P.R., GIRARD A., TESSEIR M. *et al.*, "Characterizaton of pulsed laser deposited SmFeO3 morphology: Effect of fluence, substrate temperature and oxygen pressure", *Appl. Phys A*, *Mat. Sc. Process*, vol. 79, pp. 1399–1403, 2004.

[DAH 04b] DAHOO P.R., HAMON T., NEGULESCU B. *et al.*, "Evidence by spectroscopic ellipsometry of optical property change in pulsed laser deposited NiO films when heated in air at Neel temperature", *Appl. Phys. A*, *Mat. Sci. Process*, vol. 79, pp. 1439–1443, 2004.

[DAH 06] DAHOO P.R., LAKHLIFI A., CHABBI H. *et al.*, "Matrix effect on triatomic CO_2 molecule: Comparison between krypton and xenon", *J. Mol. Struct.*, vol. 786, pp. 157–167, 2006.

[DAH 11] DAHOO P.R., "Metrological applications of ellipsometry", *Proceedings of 3rd International Metrology Conference 18–23 April 2010 (CAFMET 2010) Cairo, Egypt*, Curran Associates, Inc., September 2011.

[DAH 16] DAHOO P.R., POUGNET P., EL HAMI A., *Nanometer-scale Defect Detection Using Polarized Light*, ISTE Ltd, London and John Wiley & Sons, New York, 2016.

[DAH 17] DAHOO P.R., LAKHLIFI A., *Infrared Spectroscopy of Diatomics for Space Observation 1*, ISTE Ltd, London, and John WIley & Sons, New York, 2017.

[DAH 19] DAHOO P.R., LAKHLIFI A., *Infrared Spectroscopy of Diatomics for Space Observation 2*, ISTE Ltd, London, and John WIley & Sons, New York, 2019.

[DAH 21] DAHOO P.R., LAKHLIFI A., *Infrared Spectroscopy of Symmetric and Spherical Top Molecules for Space Observation 1*, ISTE, London, and John Wiley & Sons, New York, 2021.

[DIJ 87] DIJKAMP D., VENKATESAN T., WU X.D. *et al.*, "Preparation of Y-Ba-Cu oxide superconductor thin films using pulsed laser evaporation from high Tc bulk material", *Appl. Phys. Lett.*, vol. 51, pp. 619–621, 1987.

[DUP 06] DUPAS C., HOUDY P., LAHMANI M., *Nanoscience, Nanotechnologies and Nanophysics*, p. 823, Springer-Verlag Berlin and Heideberg GmbH & Co Eds, 2006.

[FIS 88] FISCHER E., DÜRIG U., POHL D., "Near-field scanning optical microscopy in reflection", *Appl. Phys. Lett.,* vol. 52, pp. 249–251, 1988.

[FRA 05] FRANTA D., NEGULESCU B., THOMAS L. *et al.*, "Optical properties of NiO thin films prepared by pulsed laser deposition technique", *Appl. Surf. Sci.*, vol. 244, p. 426, 2005.

[GÉR 96] GÉRADIN M., RIXEN D., *Théorie des vibrations : application à la dynamique des structures*, Masson, Paris, 1996.

[HAM 06] HAMON T., BUIL S., POPOVA E. *et al.*, "Investigation of a one dimensional magnetophotonic crystal for the study of ultrathin magnetic layer", *J. Phys. D: Appl. Phys.*, vol. 39, pp. 1–6, 2006.

[HAM 07] HAMON T., Cristaux Magnéto-photonique Unidimensionnels: Etude du Magnétisme de Couches Ultra-minces d'Oxydes, PhD thesis, Paris XI, Orsay, 2007.

[HEC 05] HECHT E. *Optics*, Pearson Education Berlin, 4th edition, 2005.

[HER 45] HERZBERG G., *Molecular Spectra and Molecular Structure II: Infrared and Raman Spectra of Polyatomic Molecules*, volume 2, Van Nostrand D. (ed.), 1945.

[KHE 14] KHETTAB M., *Etude de l'influence du résinage au niveau de L'IML (Insulated Metal Leadframe)*, *dans le packaging de module commutateur de courant mécatronique*, Thesis, UVSQ, Versailles, 2014.

[KIT 80] KITTEL C., KROEMER H., *Thermal Physics*, W.H. Freeman and Company, New York, 1980.

[KNE 20] KNEISSL M., KNORR A., REITZENSTEIN S. *et al*., *Semiconductor Nanophotonics*, p.556, Springer Nature Switzerland Eds, 2020.

[LAH 04] LAHMANI M., DUPAS C., HOUDY P., *Les nanosciences 1, nanotechnologies et nanophysqiue*, p. 718, Editions Belin, Paris, 2004.

[LAH 06] LAHMANI M., BRECHIGNAC C., HOUDY P., *Les nanosciences 2, nanomatériaux et nanochimie*, p. 26876, Editions Belin, Paris, 2006.

[LAH 07] LAHMANI M., BOISSEAU P., HOUDY P., *Les nanosciences 3, nanobiotechnologies et nanobiologie*, p. 688, Editions Belin, Paris, 2007.

[LAH 10] LAHMANI M., BOISSEAU P., HOUDY P., *Les nanosciences 4, nanotoxicologie et nanoéthique*, p. 608, Editions Belin, Paris, 2010.

[LAN 67] LANDAU L., LIFCHITZ E., *Théorie de l' élasticité*, URSS, Editions MIR, Moscow, 1967.

[LAP 94] LAPLACE P.S., *Oeuvres complètes de laplace*, volume 10, M DCCC XCIV, Editions Académies des Sciences, Gauthiers-Villars et fils imprimeurs de l'Ecole Polytechnique, Paris, 1894.

[LEE 20] LEE Y-C., MOON J-Y, *Introduction to Bionanotechnology*, p. 247, Springer-Verlag, GmbH & Co Editions, Berlin and Heideberg, 2020.

[LEW 83] LEWIS A., ISAACSON M., HAROOTUNIAN A. *et al.*, "Scanning optical spectral microscopy with 500å resolution", *Biophys. J.*, vol. 41, pp. 405a–XXX, 1983.

[LIP 81a] LIPPMANN G., "Principe de la conservation de l'électricité", *Annales de chimie et de physique*, vol. 24, pp. 145–178, 1881.

[LIP 81b] LIPPMANN G., "Principe de la conservation de l'électricité ou second principe de la théorie des phénomènes élecriques", *J. Phys. Theor. Appl.*, vol. 10, pp. 381–394, 1881.

[LOU 16] LOURTIOZ J., LAHMANI M., DUPAS-HAEBERLIN C. *et al.*, *Nanosciences and Nanotechnology: Evolution or Revolution?*, Springer International Publishing Editions, p. 438, 2016.

[LOU 18] LOURTIOZ J., VAUTRIN-UL, C., PALACIN, S. *et al.* (2018). Comprendre les Nanosciences – Session 2, available at: https://www.fun-mooc.fr/courses/course-v1:UPSUD+42003+session02/about, 2018.

[MAR 90] MARSHALL S., SKITEK G., *Electromagnetic Concepts and Applications,* Prentice Hall Inc., Englewood Cliffs, New Jersey, 1990.

[MAX 54] MAXWELL J.C., *A Treatise on Electricity and Magnetism*, 3rd edition, Dover Publications, New York, 1954.

[MEI 15] MEIS C., *Light and Vacuum*, World Scientific Publishing Co., Pte. Ltd, Singapore, 2015.

[MES 64] MESSIAH A., *Mécanique quantique*, vols 1 and 2, Dunod, Paris, 1964.

[MOH 10] MOHSINE A., EL HAMI A., "A robust study of reliability-based optimization methods under eigen-frequency", *Computer Methods in Applied Mechanics and Engineering*, vol. 199, issue 17–20, pp. 17–201006, 2010.

[MOO 65] MOORE G.E., "Cramming more components onto integrated circuit", *Electronics*, vol. 38, no. 8, 1965.

[NOU 07] NOUN W., BERINI B., DUMONT Y. *et al.*, "Correlation between electrical and ellipsometric properties on high-quality epitaxial thin films of the conductive oxide LaNiO3 on STO (001)", *Journal of Applied Physics*, vol. 102, pp. 063709/1–063709/7, 2007.

[NYE 61] NYE J.F., *Propriétés physiques des Cristaux, leur représentation par des tenseurs et des matrices*, translated by BLANC D. and PUJOL T., Dunod, Paris, 1961.

[POH 84] POHL D.W., DENK W., LANZ M., "Optical stethoscopy: Image recording with resolution λ/20", *Appl. Phys. Lett.*, vol. 44, pp. 651–653, 1984.

[POH 86] POHL D.W., Optical near field scanning microscope, US Patent 4,604,520, 1986.

[POH 87] POHL D.W., Optical near field scanning microscope, European Patent EP0112401, US Patent US 4604520, May 22, 1987.

[POU 20] POUGNET P., DAHOO P.R., ALVAREZ J.P., "Highly accelerated testing", in POUGNET P., EL HAMI A. (eds), *Embedded Mechatronic Systems 2*, Revised and Updated 2nd Edition, ISTE Press Ltd, London and Elsevier Ltd, Oxford, 2020.

[PRI 62] PRIGOGINE I., *Introduction to Thermodynamics of Irreversible Processes*, John Wiley & Sons Inc, New York, 1962.

[RAT 02] RATNER M., RATNER D., *Nanotechnology: A Gentle Introduction to the Next Big Idea*, Prentice Hall Editions, p. 208, 2003.

[RED 89] REDDICK R.C., WARMACK R.J., FERREL T.L., "New form of scanning optical microscopy", *Phys. Rev. B*, vol. 39, pp. 767–770, 1989.

[RIT 08] RITZ W., "Uber eine neue Methode zur Lösung gewisser Variationsprobleme der mathematischen Physik", *J. Reine Angew. Math.*, issue 135, pp. 1–61, 1908.

[RUS 33] RUSKA E., "Imaging of surfaces which reflect electrons in the electron microscope", *Z. Phys.*, vol. 83, pp. 492–497, 1933.

[SHO 49] SHOCKLEY W., "The theory of p-n junctions in semiconductors and p-n junction transistors", *Bell Syst. Tech. J.*, no. 28, pp. 435–489, 1949.

[SIL 49] SILVER S., *Microwave Antenna Theory and Design*, McGraw-Hill Book Co. New York, USA, 1949.

[SMI 65] SMITH H.M., TURNER A.F., "Vacuum deposited thin films using a ruby laser", *Appl. Opt.*, vol. 4, pp. 147–148, 1965.

[SYN 28] SYNGE E.H., "Suggested method for extending microscopic resolution into the ultramicroscopic region", *Phil. Mag.*, vol. 6, pp. 356–362, 1928.

[SYN 32] SYNGE E.H., "An application of piezoelectricity to microscopy", *Phil. Mag.*, vol. 13, pp. 297–300, 1932.

[TAN 74] TANIGUCHI N., " On the basic concept of 'Nano-Technology'", *Proc. Intl. Conf. Prod. Eng.*, *Part II*, Japan Society of Precision Engineering, Tokyo,1974.

[VOI 10] VOIGT, W., *Lehrbuch der Kristallphysik*. Teubner Verlag, Leipzig, 1910.

[VOI 28] VOIGT, W., *Lehrbuch der Kristallphysik*. Teubner Verlag, Leipzig, 1928.

Index

Other titles from

iSTE

in

Mechanical Engineering and Solid Mechanics

2020

SALENÇON Jean
Elastoplastic Modeling

2019

BAYLE Franck
Reliability of Maintained Systems Subjected to Wear Failure Mechanisms:
Theory and Applications
(Reliability of Multiphysical Systems Set – Volume 8)

BEN KAHLA Rabeb, BARKAOUI Abdelwahed, MERZOUKI Tarek
Finite Element Method and Medical Imaging Techniques in Bone
Biomechanics
(Mathematical and Mechanical Engineering Set – Volume 8)

IONESCU Ioan R., QUEYREAU Sylvain, PICU Catalin R., SALMAN Oguz Umut
Mechanics and Physics of Solids at Micro- and Nano-Scales

LE VAN Anh, BOUZIDI Rabah
Lagrangian Mechanics: An Advanced Analytical Approach

BOUVET Christophe
Mechanics of Aeronautical Solids, Materials and Structures
Mechanics of Aeronautical Composite Materials

BRANCHERIE Delphine, FEISSEL Pierre, BOUVIER Salima,
IBRAHIMBEGOVIC Adnan
From Microstructure Investigations to Multiscale Modeling:
Bridging the Gap

CHEBEL-MORELLO Brigitte, NICOD Jean-Marc, VARNIER Christophe
From Prognostics and Health Systems Management to Predictive
Maintenance 2: Knowledge, Traceability and Decision
(Reliability of Multiphysical Systems Set – Volume 7)

EL HAMI Abdelkhalak, RADI Bouchaib
Dynamics of Large Structures and Inverse Problems
(*Mathematical and Mechanical Engineering Set – Volume 5*)
Fluid-Structure Interactions and Uncertainties: Ansys and Fluent Tools
(Reliability of Multiphysical Systems Set – Volume 6)

KHARMANDA Ghias, EL HAMI Abdelkhalak
Biomechanics: Optimization, Uncertainties and Reliability
(Reliability of Multiphysical Systems Set – Volume 5)

LEDOUX Michel, EL HAMI Abdelkhalak
Compressible Flow Propulsion and Digital Approaches in Fluid Mechanics
(Mathematical and Mechanical Engineering Set – Volume 4)
Fluid Mechanics: Analytical Methods
(Mathematical and Mechanical Engineering Set – Volume 3)

MORI Yvon
Mechanical Vibrations: Applications to Equipment

2016

BOREL Michel, VÉNIZÉLOS Georges
Movement Equations 1: Location, Kinematics and Kinetics
(Non-deformable Solid Mechanics Set – Volume 1)

2015

KARLIČIĆ Danilo, MURMU Tony, ADHIKARI Sondipon, MCCARTHY Michael
Non-local Structural Mechanics

SAB Karam, LEBÉE Arthur
Homogenization of Heterogeneous Thin and Thick Plates

2014

ATANACKOVIC M. Teodor, PILIPOVIC Stevan, STANKOVIC Bogoljub, ZORICA Dusan
Fractional Calculus with Applications in Mechanics: Vibrations and Diffusion Processes
Fractional Calculus with Applications in Mechanics: Wave Propagation, Impact and Variational Principles

CIBLAC Thierry, MOREL Jean-Claude
Sustainable Masonry: Stability and Behavior of Structures

ILANKO Sinniah, MONTERRUBIO Luis E., MOCHIDA Yusuke
The Rayleigh−Ritz Method for Structural Analysis

LALANNE Christian
Mechanical Vibration and Shock Analysis – 5-volume series – 3rd edition
Sinusoidal Vibration – Volume 1
Mechanical Shock – Volume 2
Random Vibration – Volume 3
Fatigue Damage – Volume 4
Specification Development – Volume 5

LEMAIRE Maurice
Uncertainty and Mechanics

2013

ADHIKARI Sondipon
Structural Dynamic Analysis with Generalized Damping Models: Analysis

ADHIKARI Sondipon
Structural Dynamic Analysis with Generalized Damping Models:
Identification

BAILLY Patrice
Materials and Structures under Shock and Impact

BASTIEN Jérôme, BERNARDIN Frédéric, LAMARQUE Claude-Henri
Non-smooth Deterministic or Stochastic Discrete Dynamical Systems:
Applications to Models with Friction or Impact

EL HAMI Abdelkhalak, RADI Bouchaib
Uncertainty and Optimization in Structural Mechanics

KIRILLOV Oleg N., PELINOVSKY Dmitry E.
Nonlinear Physical Systems: Spectral Analysis, Stability and Bifurcations

LUONGO Angelo, ZULLI Daniele
Mathematical Models of Beams and Cables

SALENÇON Jean
Yield Design

2012

DAVIM J. Paulo
Mechanical Engineering Education

DUPEUX Michel, BRACCINI Muriel
Mechanics of Solid Interfaces

ELISHAKOFF Isaac *et al.*
Carbon Nanotubes and Nanosensors: Vibration, Buckling
and Ballistic Impact

GRÉDIAC Michel, HILD François
Full-Field Measurements and Identification in Solid Mechanics

GROUS Ammar
Fracture Mechanics – 3-volume series
Analysis of Reliability and Quality Control – Volume 1
Applied Reliability – Volume 2
Applied Quality Control – Volume 3

RECHO Naman
Fracture Mechanics and Crack Growth

2011

KRYSINSKI Tomasz, MALBURET François
Mechanical Instability

SOUSTELLE Michel
An Introduction to Chemical Kinetics

2010

BREITKOPF Piotr, FILOMENO COELHO Rajan
Multidisciplinary Design Optimization in Computational Mechanics

DAVIM J. Paulo
Biotribolgy

PAULTRE Patrick
Dynamics of Structures

SOUSTELLE Michel
Handbook of Heterogenous Kinetics

2009

BERLIOZ Alain, TROMPETTE Philippe
Solid Mechanics using the Finite Element Method

LEMAIRE Maurice
Structural Reliability

2007

GIRARD Alain, ROY Nicolas
Structural Dynamics in Industry

GUINEBRETIÈRE René
X-ray Diffraction by Polycrystalline Materials

KRYSINSKI Tomasz, MALBURET François
Mechanical Vibrations

KUNDU Tribikram
Advanced Ultrasonic Methods for Material and Structure Inspection

SIH George C. *et al.*
Particle and Continuum Aspects of Mesomechanics